Modulation of proton NMR free induction decay by spin diffusion

T. T. P. Cheung

Citation: The Journal of Chemical Physics **76**, 1248 (1982); doi: 10.1063/1.443142
View online: http://dx.doi.org/10.1063/1.443142
View Table of Contents: http://scitation.aip.org/content/aip/journal/jcp/76/3?ver=pdfcov
Published by the AIP Publishing

Modulation of proton NMR free induction decay by spin diffusion

T. T. P. Cheung[a)]

Ames Laboratory-DOE, and Department of Chemistry, Iowa State University, Ames, Iowa 50011
(Received 25 August 1981; accepted 1 October 1981)

The effects of spin diffusion on the free induction decay (FID) of protons associated with the noncrystalline domains of two polymers, polyethylene and blended Nylon 66 (ZYTEL-408), have been examined using Goldman–Shen NMR pulse sequence $[(1/2)\pi x - t_0 - (1/2)\pi\bar{x} - \tau - (1/2)\pi x - t]$ At $\tau \lesssim 100\,\mu$s, the FID is drastically distorted from the exponential form while at longer $\tau(\tau \gtrsim 500\,\mu$s) an exponential FID is observed; but its transverse spin relaxation rate is smaller than that of the FID obtained after a single $(1/2)\pi x$ pulse and approaches this value at the limit of large τ. These findings are interpreted in terms of the theory of rapid spin diffusion. The spatial variation in the spin relaxation rate within the noncrystalline domain is inferred.

I. INTRODUCTION

Spin-flip diffusion[1] leads to communication among spins at various sites in a dipolar coupled spin system. Such communication may provide useful information about the spatial inhomogeneity within the system. Based on the concept of spin-flip diffusion, we have recently[2] applied the Goldman–Shen[3] NMR pulse sequence and its modified version[4] to investigate domain structures in solid polymers.

From the NMR standpoint, spatial inhomogeneity in solid polymers may be described in terms of crystalline and noncrystalline domains. The latter domains are distinguished from the former domains by the fact that the FID $\varphi(t)$ of protons (^{1}H) associated with the latter usually has a longer transverse spin relaxation time T_2 than that associated with the former. Furthermore, $\varphi(t)$ follows the shape of an exponential decay [by this we mean a decay $\varphi(t) = \exp -(t/T_2)$], whereas that of the crystalline domains is more appropriately described by a Gaussian.

In the Goldman–Shen sequence $(\frac{1}{2}\pi x - t_0 - \frac{1}{2}\pi\bar{x} - \tau - \frac{1}{2}\pi x - t)$ we observe the FID of the resulting ^{1}H magnetization after the third pulse. The fixed t_0 is chosen such that magnetization associated with the crystalline domains has decayed to zero while there is still sufficient magnetization remaining in the noncrystalline domains. The variable time τ is the duration in which magnetization in the latter domains is allowed to diffuse to the former via dipolar spin flip. One extracts[2,5] information about domain sizes and shapes by following the recovery of the magnetization in the former domains as a function of τ. Clearly, when τ is small in comparison to the time scale of considerable spin diffusion, the FID observed after the third pulse is simply that of the noncrystalline domains which will be denoted by $\varphi(t, \tau)$.

It is important to distinguish $\varphi(t, \tau)$ created after the Goldman–Shen sequence from $\varphi(t)$ obtained after a single $(\pi/2)x$ pulse, i.e., $[(\pi/2)x - t]$, by the fact that the former has an additional dependence on τ. This distinction is necessary because different preparation pulse sequences lead to different initial $(t = 0)$ spatial distributions of the ^{1}H magnetization.

To contrast with the uniform initial $(t = 0)$ distribution in $\varphi(t)$, the $t = 0$ distribution in $\varphi(t, \tau)$ as a function of τ is depicted in Fig. 1 in a one-dimensional profile. Since the transverse spin relaxation rate in the crystalline domain is much faster than that in the noncrystalline domain and spin diffusion occurs during the time t_0, at $\tau \sim 0$ a depletion layer of thickness Δ is formed in the noncrystalline domain as shown in Fig. 1(a). Thus, there is nonuniformity in the $t = 0$ spatial distribution of ^{1}H magnetization within each domain as well as between domains of different types. The main purpose of this paper is to investigate the effects of such nonuniform distribution on the FID of the noncrystalline domains, namely, we shall examine the differences between $\varphi(t, \tau)$ and $\varphi(t)$.

One should note that in using the concept of initial $(t = 0)$ distribution of magnetization after the Goldman–Shen sequence, one is restricted to τ sufficiently long such that local equilibrium (local spin temperature) can be established at every point in the noncrystalline domain. Thus, in the following discussion, when we say $\tau \sim 0$ or $\tau \to 0$ we mean a τ much smaller than the time it takes the crystalline and noncrystalline domains to come to equilibrium, i.e., to achieve uniform magnetization, but long enough for local equilibrium to be established within the noncrystalline domain.

Recently, we have shown[6] theoretically that when there is nonuniform spatial distribution in the magnetization and the spin relaxation rate is a function of the site $\mathbf{r}$, spin diffusion couples these two spatial inhomogeneities and leads to modification of the time evolution of the magnetization. Explicitly in the case of nonuniform $1/T_2(\mathbf{r})$, denoting the local magnetization density at site $\mathbf{r}$ and time t by $M(\mathbf{r}, t, \tau)$, the spin diffusion coefficient by D and the local spin relaxation rate at site $\mathbf{r}$ by $A(\mathbf{r})$ $[A(\mathbf{r}) = 1/T_2(\mathbf{r})]$, we have found that in the rapid diffusion limit[7] the diffusion equation

$$\frac{\partial M(\mathbf{r}, t, \tau)}{\partial t} = D\nabla^2 M(\mathbf{r}, t, \tau) - A(\mathbf{r})M(\mathbf{r}, t, \tau) \qquad (1)$$

[a)] Present address: Phillips Petroleum Company, Phillips Research Center, Bartlesville, Okl. 74004.

 0021-9606/82/031248-07$02.10

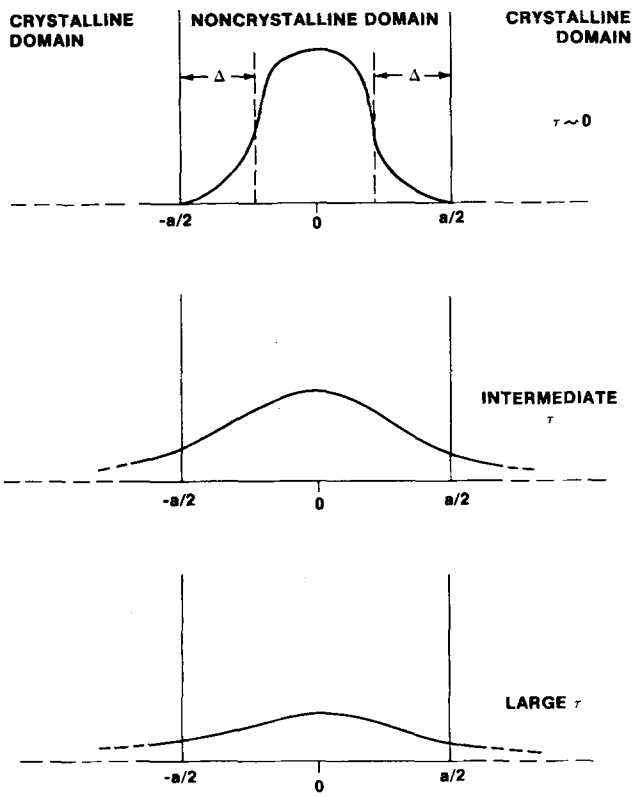

FIG. 1. The $t=0$ spatial distribution of ^{1}H magnetization as a function of τ.

leads[8] to $\varphi(t, \tau)$ of the form

$$\varphi(t, \tau) = \varphi(t) + \tilde{\varphi}(t, \tau) , \tag{2}$$

$$\varphi(t) = M_{q=0}(t=0, \tau) \exp(-\Lambda_{q=0} t) , \tag{3}$$

$$\tilde{\varphi}(t, \tau) = V^{-1} \sum_{q \neq 0} \frac{\delta A(-q)}{Dq^2} \times M_q(t=0, \tau)[\exp(-\Lambda_q t) - \exp(-\Lambda_{q=0} t)] . \tag{4}$$

We have defined

$$M(\mathbf{r}, t=0, \tau) \equiv \sum_q M_q(t=0, \tau) \exp(i\mathbf{q}\cdot\mathbf{r}) , \tag{5}$$

$$\delta A(\mathbf{q}) \equiv \int d\mathbf{r} \exp(-i\mathbf{q}\cdot\mathbf{r}) \left[A(\mathbf{r}) - V^{-1}\int d\mathbf{r}\, A(\mathbf{r})\right] \equiv \int d\mathbf{r} \exp(-i\mathbf{q}\cdot\mathbf{r})\, \delta A(\mathbf{r}) , \tag{6}$$

$$\Lambda_q = V^{-1}\int d\mathbf{r}\, A(\mathbf{r}) + Dq^2 + V^{-2} \sum_{q'(\neq q)} \frac{|\delta A(\mathbf{q}' - \mathbf{q})|^2}{D(q^2 - q'^2)} . \tag{7}$$

The volume integration $\int d\mathbf{r}$ is taken over the volume V of the noncrystalline domain. The dependence of the initial ($t=0$) condition of Eq. (1) on τ is explicitly indicated in Eq. (5). For convenience, we shall denote $M(\mathbf{r}, t=0, \tau)$ and $M_q(t=0, \tau)$ by $M(\mathbf{r}, \tau)$ and $M_q(\tau)$, respectively.

When $M(\mathbf{r}, \tau)$ is uniform throughout the noncrystalline domain V, i.e., $M_q(\tau)=0$ for all $\mathbf{q}\neq 0$, then $\varphi(t, \tau) = \varphi(t)$ with $1/T_2(\tau)$ given by Λ_0. Thus, coupling of the spatial inhomogeneities in $M(\mathbf{r}, \tau)$ and $A(\mathbf{r})$ leads to the contribution of $\tilde{\varphi}(t, \tau)$ to $\varphi(t, \tau)$. The significance of the contribution depends on the degree of the spatial inhomogeneities.

In this paper we shall examine two polymers—polyethylene (PE) and a blended Nylon 66(Zytel-408). The principal results are (1) $\varphi(t, \tau)$ is drastically distorted from the exponential $\varphi(t)$ when $\tau \lesssim 100$ μs, and (2) when $\tau \gtrsim 500$ μs, $\varphi(t, \tau)$ begins to taken on the exponential form but its relaxation rate $1/T_2(\tau)$ is smaller than that of $\varphi(t)$ and approaches to this value in the limit of large τ. These findings will be interpreted qualitatively in terms of the theory of rapid spin diffusion.

II. EXPERIMENTAL

^{1}H NMR spectra were obtained using a fast-recovery multipulse NMR spectrometer[9] which operates at 55.37 MHz for ^{1}H. A standard probe with a series tapped tuned circuit was used for all measurements. The pulse width of the $(\pi/2)$ pulse was 1.2 μs and the receiver recovery time was roughly 3.5 μs.

The characterization of the polyethylene (PE) has been described elsewhere.[2] Briefly, it has a crystallinity of 65%, a number average molecular weight of 8120, and a weight average molecular weight of 135 000. The blended Nylon 66 (Zytel-408) was provided by Larry Ryan of DuPont. It consists of 20% Surylan.

The NMR parameters of both materials are tabulated in Table I. The FID of each polymer after a single $(\pi/2)x$ pulse exhibits a two component decay. Two distinct transverse relaxation times can be obtained by nonlinear least square fitting of the decay to a fast Gaussian and a slow exponential decay.

Similarly, at long τ ($\tau > 1$ ms) the FID after the Goldman–Shen sequence can be decomposed into a fast Gaussian and a slow exponential. The decay rate of the exponential component gives $1/T_2(\tau)$ of $\varphi(t, \tau)$.

III. RESULTS AND DISCUSSION

The experimental results of the transverse relaxation rates $1/T_2(\tau)$ of $\varphi(t, \tau)$ as a function of τ are shown in Fig. 2. t_0 of 42 and 40 μs were chosen for PE and Zytel-408, respectively. It is clear that $1/T_2(\tau)$ of each polymer increases as the diffusion time τ increases and approaches the value of that of $\varphi(t)$ at the limit of large τ. In other words, at small τ, $T_2(\tau)$ is lengthened in comparison to that of $\varphi(t)$. Our observation is consistent with Assink's results[5] on polyurethane.

TABLE I. The NMR parameters of the materials studied.

	Transverse relaxation times (μs)		% Fast Gaussian component	T_1 (s)
	Fast Gaussian	Slow exponential		
Polyethylene	7.3 ± 0.3	35 ± 1	78	0.45
Zytel-408	8.7 ± 0.4	42 ± 2	93	0.24

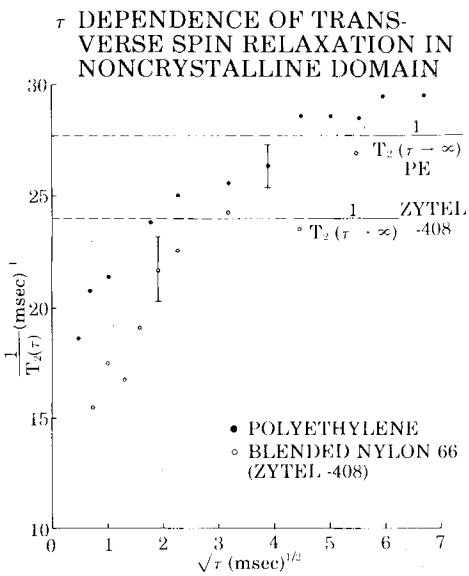

FIG. 2. The transverse spin relaxation rate $1/T_2(\tau)$ of $\varphi(t,\tau)$ as a function of τ.

The time (t) evolution of the FID of the total magnetization after the Goldman–Shen sequence as a function of τ are shown in Figs. 3 and 4, respectively, for PE and Zytel-408. At these values of τ ($\tau \lesssim 500$ μs), spin diffusion between the noncrystalline and crystalline domains is rather limited. Thus, in practical terms, the observed FID is essentially $\varphi(t,\tau)$.

The distortion of $\varphi(t,\tau)$ from the exponential $\varphi(t)$ is featured with hump and depression. It follows a similar pattern in both polymers: (1) At $\tau\sim500$ μs, an approximately exponential $\varphi(t,\tau)$ is observed. (2) At $\tau\sim100$ μs, a hump (indicated by L1 in the figures) begins to develop. It becomes more conspicuous at $\tau\sim50$ μs. (3) At even smaller τ, a depression (indicated by L2 in the figures) begins to appear at the location between the hump L1 and the origin of the decay. It drastically attenuates the decay and now part of $\varphi(t,\tau)$ becomes negative. This can be clearly seen at $\tau\sim10$ μs. The integration of $\varphi(t,\tau)$ over t indicates that the area of $\varphi(t,\tau\sim100$ μs) is larger, whereas that of $\varphi(t,\tau\sim10$ μs) is smaller than that of $\varphi(t)$.

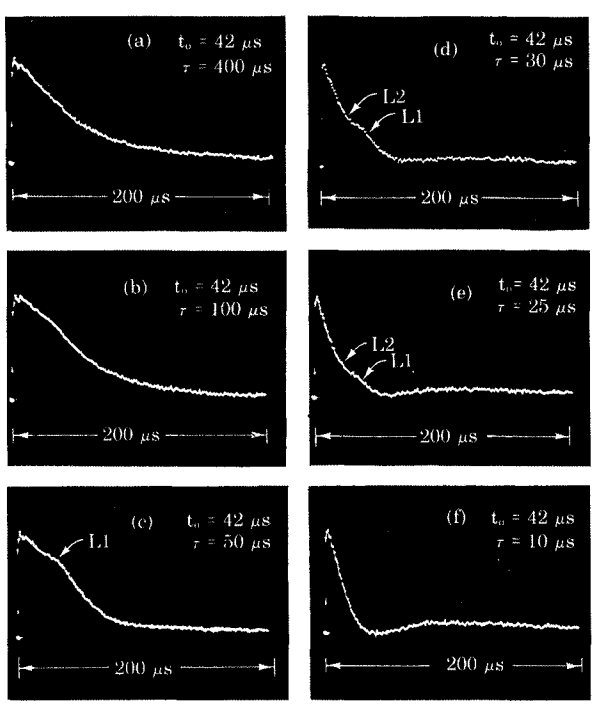

FIG. 3. The time (t) evolution of the FID of polyethylene after the Goldman–Shen sequence as a function of τ.

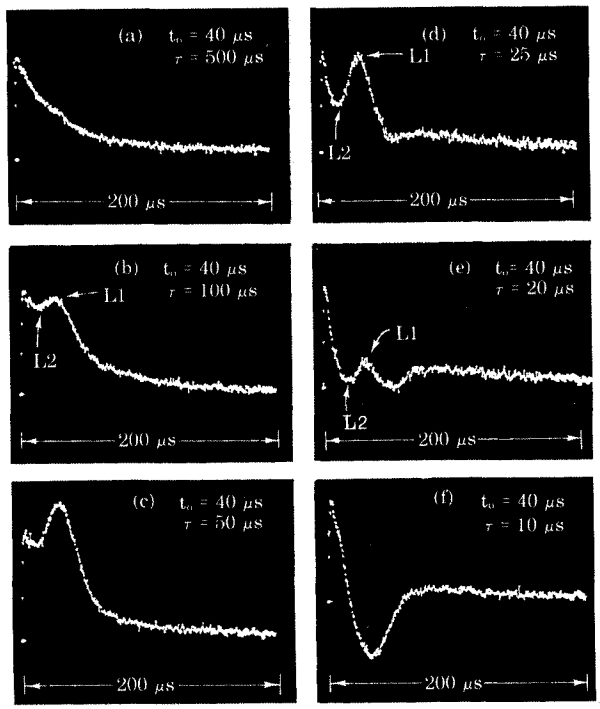

FIG. 4. The time (t) evolution of the FID of Zytel-408 after the Goldman–Shen sequence as a function of τ.

The shape of $\varphi(t,\tau)$ also varies as a function of t_0. $\varphi(t,\tau)$ of Zytel-408 with $t_0=60$ μs and $\tau=50$ μs is shown in Fig. 5. It should be contrasted with $t_0=40$ μs and $\tau=50$ μs in Fig. 4(c). There is a general trend that as t_0 increases the development of the hump L1 and depression L2 are suppressed.

In order to assure that our results were not caused by instrumental artifice, similar experiments were performed on a distilled water sample where there is no spatial inhomogeneity in the initial magnetization (except that due to static field inhomogeneity) and the dipolar interactions are motionally averaged to zero.

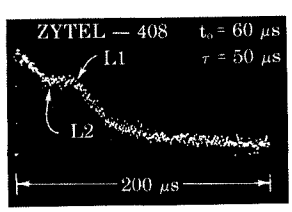

FIG. 5. The time (t) evolution of the FID of Zytel-408 after the Goldman–Shen sequence with $t_0=60$ μs and $\tau=50$ μs.

Here we did not observe any distortion in $\varphi(t, \tau)$. Furthermore, some of our results have already been confirmed. In particular, R. E. Taylor has repeated our experiments on a polyethylene sample of his own using a Bruker CXP 200 NMR spectrometer and C. G. Fry has examined some fluorinated materials as well as confirmed some of our results of the Zytel sample.

In the following we shall attempt to interpret our results in terms of the theory of rapid spin diffusion outlined in the Introduction. For simplicity, we shall treat the problem in one dimension and assume that spatial properties of the system are even with respect to $x=0$, as shown in Fig. 1 for the distribution of ^{1}H magnetization.

The contribution of $\tilde{\varphi}(t, \tau)$ to $\varphi(t, \tau)$ is determined by $M_q(\tau)$ and $\delta A(q)$, where each wave vector q is any integer n times $2\pi/a$. Using the even spatial symmetry we have

$$M(x, \tau) = M_{n=0}(\tau) + \sum_{n=1}^{\infty} M_n(\tau) \cos \frac{2\pi n x}{a} , \quad -a/2 \le x \le a/2 , \tag{8}$$

$$\delta A(x) = \sum_{n=1}^{\infty} \delta A_n \cos \frac{2\pi n x}{a} , \quad -a/2 \le x \le a/2 . \tag{9}$$

To estimate $M_n(\tau)$ as $\tau \to 0$, we shall approximate the distribution of $M(x, \tau \sim 0)$ by

$$M(x, \tau) = \exp\left[-\left(\frac{x}{a/2 - \Delta}\right)^2\right] , \quad (a/2) - \Delta \lesssim \Delta . \tag{10}$$

Δ is defined in Fig. 1 as the thickness of the depletion layer. Then it follows[10] that

$$M_{n=0}(\tau \sim 0) = \frac{\sqrt{\pi}}{2} \xi , \tag{11}$$

$$M_{n\neq 0}(\tau \sim 0) = \sqrt{\pi}\, \xi \exp\left[-\left(\frac{\pi n \xi}{2}\right)^2\right] , \tag{12}$$

where $\xi \equiv [(a - 2\Delta)/a]$. One should note

$$M_n(\tau \sim 0) > 0 . \tag{13}$$

Furthermore, when $\xi \ll 1$, one has

$$M_1(\tau \sim 0) \simeq M_2(\tau \sim 0) . \tag{14}$$

Relation (13) also holds for nonzero τ so long as τ is sufficiently short such that Eq. (10) is appropriate. Moreover, $M_{n=1}(\tau)$ is always positive for arbitrary τ, as expected from Fig. 1.

Since at large τ the deviation of $M(x, \tau)$ from the uniform distribution is small, we can always expand $M(x, \tau)$ in powers of x^2. To the first order, one obtains

$$M(x, \tau) = P(\tau) - Q(\tau) x^2 , \quad -a/2 \le x \le a/2 , \tag{15}$$

where $Q(\tau) \ge 0$ and $Q(\tau) \to 0$ as $\tau \to \infty$. Now the Fourier components become

$$M_0(\tau) = P(\tau) - Q(\tau) a^2/12 , \tag{16a}$$

$$M_{n\neq 0}(\tau) = (-1)^{n+1} \left(\frac{a}{\pi n}\right)^2 Q(\tau) . \tag{16b}$$

Thus, at large τ, $M_{n=1}(\tau)$ will always dominate over $M_{n\ge 2}(\tau)$ terms. One should observe that now $M_{n=1}(\tau) > 0$, whereas $M_{n=2}(\tau) < 0$.

Determination of δA_n's requires the knowledge of the spatial dependence of $\delta A(x)$, though we do not usually have such information. Nevertheless, $\delta A(x)$ is expected to vary smoothly across the interval $(-a/2, a/2)$; it is not unreasonable to assume that δA_1 and δA_2 suffice for $\delta A(x)$. Then, Eq. (4) reduces to

$$\tilde{\varphi}(t, \tau) = \tilde{\varphi}_1(t, \tau) + \tilde{\varphi}_2(t, \tau) , \tag{17}$$

with

$$\tilde{\varphi}_1(t, \tau) = \frac{\delta A_1 a^2}{4\pi^2 D} M_1(\tau)[\exp(-\Lambda_1 t) - \exp(-\Lambda_0 t)] , \tag{18}$$

and

$$\tilde{\varphi}_2(t, \tau) = \frac{\delta A_2 a^2}{16\pi^2 D} M_2(\tau)[\exp(-\Lambda_2 t) - \exp(-\Lambda_0 t)] . \tag{19}$$

Furthermore, the general expectation that the packing of polymer chains in the noncrystalline domain is more dense at the region close to the crystalline domain than that at the center suggests[11] that $\delta A_1 < 0$ and $\delta A_2 > 0$. This follows from the fact that a looser packing indicates larger distances between protons and increase of free volume for librational motions of the polymer segments. Both have the effects of reducing the dipolar interactions between protons, thus leading to a smaller $A(\mathbf{r})$. The conditions $\delta A_1 < 0$ and $\delta A_2 > 0$ are also essential to the interpretation of the data in Figs. 3 and 4, described below.

The decrease of the transverse relaxation rate shown in Fig. 2 can be understood as the following: Using Eq. (17), Eq. (2) can be rewritten as

$$\varphi(t, \tau) = M_0(\tau) \exp(-\Lambda_0 t) \left(1 + \sum_{n=1}^{2} \frac{\delta A_n a^2}{(2\pi n)^2 D} \cdot \frac{M_n(\tau)}{M_0(\tau)} \times \{\exp[-(\Lambda_n - \Lambda_0)t] - 1\}\right) . \tag{20}$$

It has been shown[2,12] that for PE and Zytel-408, $a^2/D > 1$ ms. Thus, for t on the order of $\Lambda_0^{-1} \sim T_2$,

$$(\Lambda_n - \Lambda_0)t \simeq \left(\frac{2\pi n}{a}\right)^2 Dt \ll 1$$

and Eq. (20) reduces to

$$\varphi(t, \tau) = M_0(\tau) \exp(-\Lambda_0 t) \left[1 - t \sum_{n=1}^{2} \delta A_n M_n(\tau)/M_0(\tau)\right] = M_0(\tau) \exp\left\{-\left[\Lambda_0 + \sum_{n=1}^{2} \delta A_n M_n(\tau)/M_0(\tau)\right] t\right\} . \tag{21}$$

The second equality follows from the fact $[M_n(\tau)/M_0(\tau)] \ll 1$ when τ is large. The transverse relaxation time $T_2(\tau)$ of $\varphi(t, \tau)$ is defined as

$$T_2^{-1}(\tau) = T_2^{-1}(\tau \to \infty) + \sum_{n=1}^{2} \delta A_n M_n(\tau)/M_0(\tau) , \tag{22}$$

where $T_2(\tau \to \infty) \equiv \Lambda_0^{-1}$ is the transverse relaxation time of $\varphi(t)$. Since we have argued that $\delta A_1 < 0$ and $\delta A_2 > 0$, whereas $M_1(\tau) > 0$ and $M_2(\tau) < 0$ at large τ, $T_2^{-1}(\tau)$ is always smaller than $T_2^{-1}(\tau \to \infty)$. Moreover, $[M_{n\neq 0}(\tau)/M_0(\tau)] \to 0$ as τ increases. Therefore, $T_2^{-1}(\tau)$ approaches $T_2^{-1}(\tau \to \infty)$ at the limit of large τ.

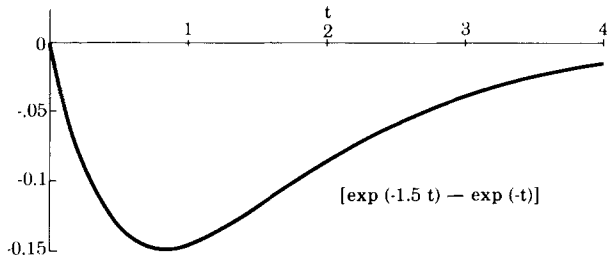

FIG. 6. $[\exp(-1.5t)-\exp(-t)]$ as a function of t.

We believe that our observation of $T_2^{-1}(\tau) \leq T_2^{-1}(\tau \to \infty)$ is a general phenomenon in materials with $\delta A_1 < 0$ and $|\delta A_1| \gtrsim |\delta A_{n>1}|$ because at large τ only $M_1(\tau)$ is important and $M_1(\tau) > 0$. Therefore, only $\delta A_1 M_1(\tau)/M_0(\tau) < 0$ in the second term contributes most to Eq. (22).

In order to be consistent with the data in Figs. 3 and 4, δA_1 and δA_2 must satisfy the following conditions: (1) $\delta A_1 < 0$, $\delta A_2 > 0$ and (2) $|\delta A_2| \gtrsim 4|\delta A_1|$ though the first condition has already been suggested on physical grounds. To see this, we first observe that $\Lambda_n > \Lambda_0$ and hence $[\exp(-\Lambda_n t) - \exp(-\Lambda_0 t)] < 0$ for all t as shown schematically in Fig. 6. Second, the minimum of the curve shifts toward $t = 0$ as n increases.

Now, according to Figs. 3 and 4, at large τ ($\tau \sim 500$ μs), the fact that the area under $\varphi(t, \tau)$ is larger than that of $\varphi(t)$ demands $\int \tilde{\varphi}(t, \tau) dt > 0$. Since we have shown that $M_1(\tau) > 0$ while $M_2(\tau) < 0$ at large τ, then according to Eq. (17) [or Eq. (20)] the conditions $\delta A_1 > 0$ and $\delta A_2 < 0$ are not allowed. In the remaining combinations ($\delta A_1 < 0$, $\delta A_2 > 0$; $\delta A_1 > 0$, $\delta A_2 > 0$ and $\delta A_1 < 0$, $\delta A_2 < 0$) the last combination can also be ruled out because at small τ we have, from Eq. (12), $M_1(\tau) > 0$ and $M_2(\tau) > 0$. The conditions $\delta A_1 < 0$ and $\delta A_2 < 0$ would have led to $\tilde{\varphi}(t, \tau) > 0$ for all t; hence, $\int \tilde{\varphi}(t, \tau) dt > 0$, which contradicts our observation of $\int \tilde{\varphi}(t, \tau) < 0$ [i.e., $\int \varphi(t, \tau) dt < \int \varphi(t) dt$] at small τ. Finally, the occurrence of the depression L2 together with the hump L1 indicates that only the first condition is permissible.

The condition $|\delta A_2| \geq 4|\delta A_1|$ follows from the fact that part of $\varphi(t, \tau)$ may become negative at small τ as shown in Figs. 3(f) and 4(f).

The above interpretation is also consistent with the re-

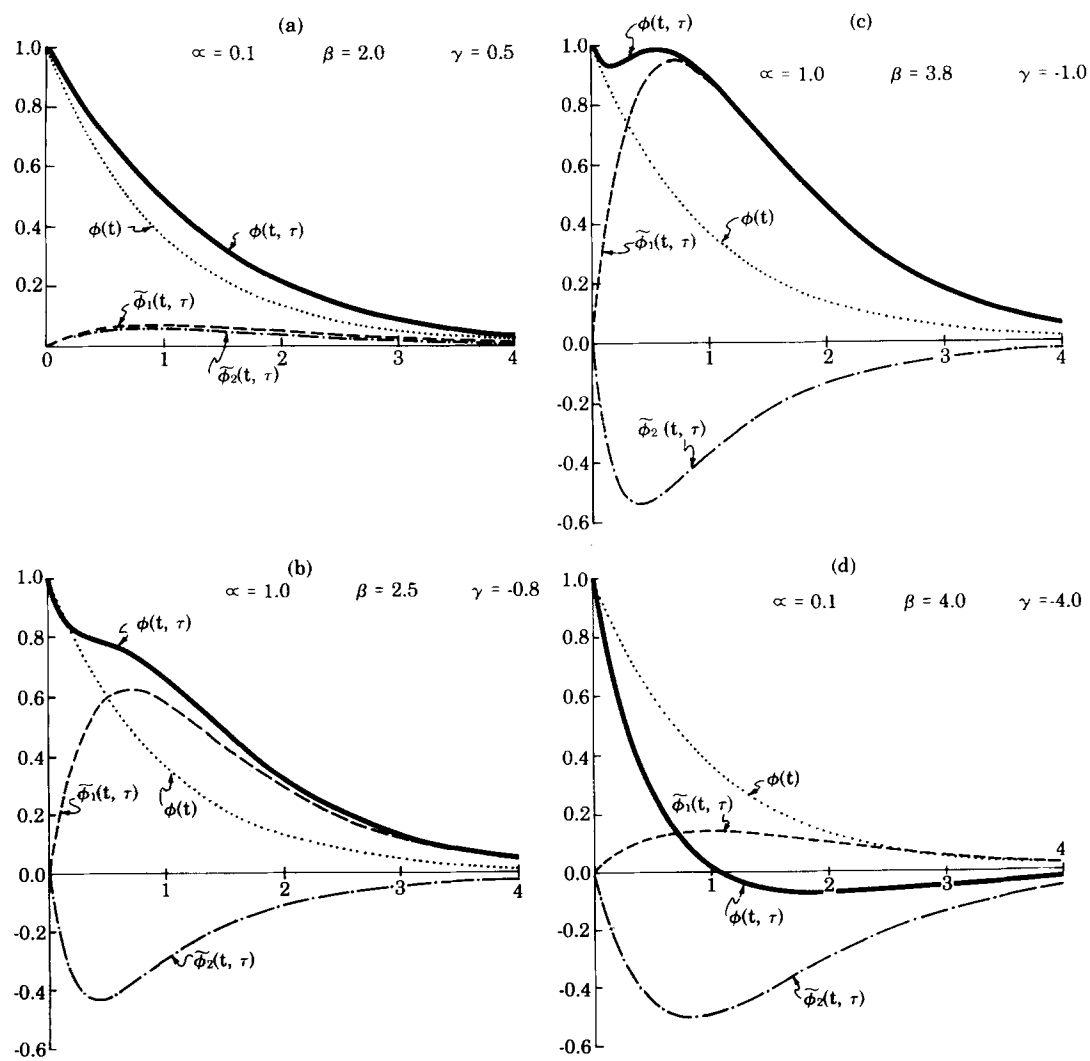

FIG. 7. $\exp(-t)\{1+\beta[1-\exp(-\alpha t)]+\gamma[1-\exp(-4\alpha t)]\}$ as a function of t with various α, β, and γ.

sults in Fig. 5. As t_0 increases, sufficient time is allowed for ^{1}H magnetization from the center of the noncrystalline domain to diffuse to the depletion layer created at shorter t_0. Consequently, the Fourier components $M_1(\tau)$ and $M_2(\tau)$ are smaller and make smaller contributions to $\tilde{\varphi}(t, \tau)$.

It is interesting to see if Eq. (20) can simulate the shapes of the FID's in Figs. 3 and 4. Expressing t and $\varphi(t, \tau)$, respectively, in units of Λ_0^{-1} and $M_0(\tau)$, Eq. (20) may be rewritten as

$$\varphi(t, \tau) = \exp(-t)\{1 + \beta[1 - \exp(-\alpha t)] + \gamma[1 - \exp(-4\alpha t)]\}, \quad (23)$$

where

$$\beta = -\left(\frac{\delta A_1 a^2}{4\pi^2 D}\right)\left[\frac{M_1(\tau)}{M_0(\tau)}\right] > 0,$$

$$\gamma = -\left(\frac{\delta A_2 a^2}{16\pi^2 D}\right)\left[\frac{M_2(\tau)}{M_0(\tau)}\right],$$

and

$$\alpha = \left(\frac{2\pi}{a}\right)^2 D/\Lambda_0 .$$

The approximation $(\Lambda_n - \Lambda_0) \simeq (2\pi n/a)^2 D$ has been made. $\varphi(t, \tau)$ with various α, $\beta(\beta > 0)$, and γ are shown in Fig. 7. One observes that the general features of the FID are indeed reproduced, though β and $|\gamma|$ on the order of unity are required. These values are unusually large because in the rapid spin diffusion limit $[(\delta A_n a^2/D) \ll 1]$ they imply that $[M_n(\tau)/M_0(\tau)] \gg 1$, which is quite unreasonable on physical grounds. Also, $\alpha = 1$ in Figs. 7(b) and 7(c) is rather disturbing. Using $\Lambda_0^{-1} \sim 40$ μs, this implies that $\sqrt{D/a^2} \sim 25/\text{s}^{1/2}$ but experiments[2] on PE have already indicated that $\sqrt{D/a^2} \lesssim 7/\text{s}^{1/2}$.

The failure of the theory to provide a quantitative description of the experiments may be traced back to the fact that the theory is originally developed for a solid of infinite volume[6] in which surface effects can be neglected. The validity of our extrapolation of such a theory to the situation in which the size of the system is confined to that of the noncrystalline domain which is only on the order of 100 Å is always questionable.

One may observe that in order to reproduce the FID's in Figs. 3 and 4, $\tilde{\varphi}(t, \tau)$ must have a sharp maximum and/or minimum. Our calculations have included only contributions from $\tilde{\varphi}_1(t, \tau)$ and $\tilde{\varphi}_2(t, \tau)$ which, as have been shown in Fig. 7, are rather broad and diffuse. The resulting $\tilde{\varphi}(t, \tau)$ is therefore also quite broad and does not have any sharp maximum or minimum. One may have to include higher $\tilde{\varphi}_n(t, \tau)$ terms [i.e., include higher δA_n's in $A(\mathbf{r})$] in order to produce such effects.

IV. CONCLUSION REMARKS

We have examined the effects of spin diffusion on the FID of two polymers in which there are spatial variations in the initial magnetization and in the transverse relaxation time. The significance of the distortion of the FID depends on the magnitude of both spatial inhomogeneities. An important point is that one may infer the spatial dependence of $A(\mathbf{r})$ from such distortion.

We have also studied other polymers. The deviations of $\varphi(t, \tau)$ from $\varphi(t)$ are less distinct than those reported here. This implies that the spatial distributions of $A(\mathbf{r})$ are more uniform in these materials.

Solid-echo pulse sequences[13] like $[(\pi/2)x - t_0 - (\pi/2)y - t]$ can refocus magnetization to produce a hump on the FID. In order to see whether the results in Figs. 3 and 4 may have been caused by the refocusing effect, we have performed experiments using the sequence $[(\pi/2)\bar{x} - t_0 - (\pi/2)\bar{x} - \tau - (\pi/2)\bar{x} - t]$ which have the same effect as the original Goldman-Shen pulse sequence in creating the initial spatial inhomogeneity in $M(\mathbf{r}, \tau)$. We expect that if the distortion of $\varphi(t, \tau)$ had been due to multipulse refocusing, difference in the pulse sequence would have led to different types of distortion. However, we observed the same distortion in the subsequent experiments. Thus, it is unlikely that multipulse refocusing is the cause of the changes in the shape of the FID.

It is also unlikely that multiple quantum interference discussed by Emid *et al.*[14,15] would lead to the distortion. We have measured the $\varphi(t = 0, \tau)$ as a function of τ for PE and found that it remained constant throughout the range of τ we studied. Multiple quantum interference would have led to the modulation of $\varphi(t = 0, \tau)$ as a function of τ.

Finally, we should point out that $M_2(\tau \to 0) > 0$ in relation (12) is not merely a consequence of our usage of the Gaussian distribution for $M(x, \tau \to 0)$ but rather is a necessity to describe the data in Figs. 3 and 4. Had we had $M_2(\tau \to 0) < 0$, δA_2 must have satisfied the relation $\delta A_2 < 4\delta A_1 < 0$ in order to explain the shape of the FID at small τ. However, substituting this relation into Eq. (22) leads to $T_2^{-1}(\tau) > T_2^{-1}(\tau \to \infty)$ at long τ which is in clear contradiction to the results in Fig. 2.

ACKNOWLEDGMENTS

The Ames Laboratory is operated for the U.S. Department of Energy by Iowa State University under contract No. W-7405-Eng-82. This research was supported by the Assistant Secretary for Energy Research, Office of Energy Sciences, WPAS-KC-03-02-01.

The author would like to thank C. G. Fry and R. E. Taylor for their critical comments on the manuscript as well as performing experiments to confirm some of our results.

[1] N. Bloembergen, Physica (Utrecht) **15**, 386 (1949).
[2] T. T. P. Cheung and B. C. Gerstein, J. Appl. Phys. **52**, 5517 (1981).
[3] M. Goldman and L. Shen, Phys. Rev. **144**, 321 (1966).
[4] T. T. P. Cheung, B. C. Gerstein, L. M. Ryan, R. E. Taylor, and C. R. Dybowski, J. Chem. Phys. **73**, 6059 (1980).
[5] R. A. Assink, Macromolecules **11**, 1233 (1978).
[6] T. T. P. Cheung, Phys. Rev. B **23**, 1404 (1981).
[7] The rapid diffusion limit is defined in Ref. 6 as $Dt^{-2} \gg |\Delta A|$, where l is the average distance between extrema in $A(\mathbf{r})$ and $|\Delta A|$ is the maximal variation in $A(\mathbf{r})$.
[8] To obtain Eqs. (3) and (4) from Ref. 6, one simply substitutes

Eq. (56′) there into Eq. (61) and retains terms to the first order of $[\delta A(\mathbf{q}'-\mathbf{q})/D(q^2-q'^2)]$.

[9]B. C. Gerstein, C. Chow, R. G. Pembleton, and R. C. Wilson, J. Phys. Chem. **81**, 565 (1977).

[10]Since the distribution in Eq. (10) is essentially zero for $|x| > a/2$, we may approximate the integration $\int_{-a/2}^{a/2} dx$ by $\int_{-\infty}^{\infty} dx$ in the evaluations of the Fourier components.

[11]For instance, if $\delta A(x)$ is a weak function of x, it may be expanded to the first order in x^2

$$\delta A(x) = J + Kx^2 ,$$

where $K > 0$. Then one finds, similar to Eq. (16b),

$$\delta A_{n\neq 0} = (-1)^n \left(\frac{a}{\pi n}\right)^2 K .$$

Thus, $\delta A_1 < 0$, whereas $\delta A_2 > 0$.

[12]T. T. P. Cheung (unpublished).

[13]J. G. Powles and P. Mansfield, Phys. Lett. **2**, 58 (1962).

[14]S. Emid, A. Bax, J. Konijnendijk, J. Smidt, and A. Pines, Physica (Utrecht) B **96**, 333 (1979).

[15]S. Emid, J. Konijnendijk, J. Smidt, and A. Pines, Physica (Utrecht) B **100**, 215 (1980).